

Supplemental Material

Supplemental Methods

Hepatocyte ploidy analysis

Kidney immunostaining

Plasma and urine chemistry analysis

Plasma and urine amino acid analysis

Supplemental Figures

Supplemental Figure 1 Screening for chimeric mice based on contribution of iPS cells to digits.

Supplemental Figure 2 Blood analysis of liver function parameters in mice off NTBC at P70 and P300.

Supplemental Figure 3 Hepatocyte ploidy analysis.

Supplemental Figure 4 Kidneys repopulated with iPS cell-derived proximal tubular cells provide normal function.

Supplemental Figure 5 Analysis of parameters of liver growth and function after two-thirds partial hepatectomy.

Supplemental Figure 6 Hepatocytes of Rosa26 mice can be reliably detected with X-gal staining.

Supplemental Figure 7 Visualization of blastocyst-derived hepatocytes rules out cell fusion as the mechanism underlying hepatocyte differentiation of iPS cells free of foreign DNA.

Supplemental Tables

Supplemental Table 1 Plasma amino acid levels.

Supplemental Table 2 Urine amino acid levels.

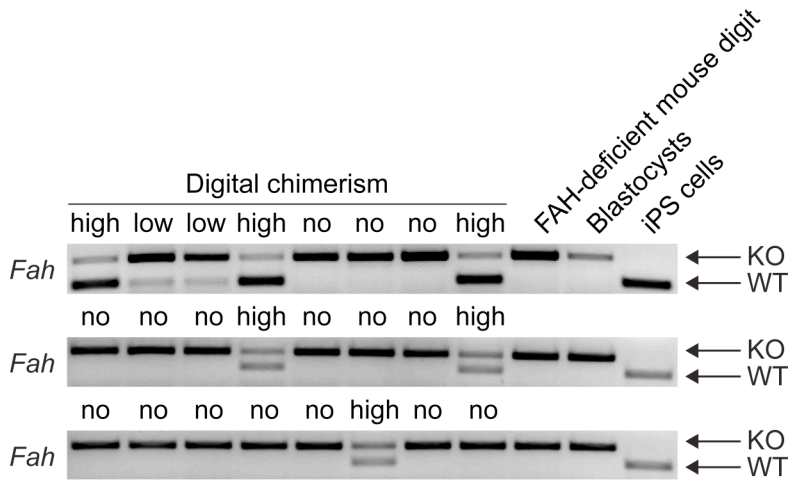
Supplemental Methods

Hepatocyte ploidy analysis. 10 μm -thick liver cryosections were stained with 2 $\mu\text{g}/\text{ml}$ 4',6-diamidino-2-phenylindole (DAPI, Molecular Probes) and z-stacks were acquired on a Leica SP5 TCS microscope at 1024 x 1024 pixels with a 63x objective. In Volocity software (Improvision), the volume of nuclei was determined in image stacks using the measurement function to select objects by fluorescence intensity and minimum size exclusion. Objects that included multiple nuclei (e.g. binucleated cells) were excluded from consideration by visual inspection and volume measurements were exported to Excel (Microsoft) for analysis. Nuclear volumes were graphed in order of increasing size and inflection points on the slope were used to determine cut-off points in ploidy between 2n, 4n and $\geq 8n$.

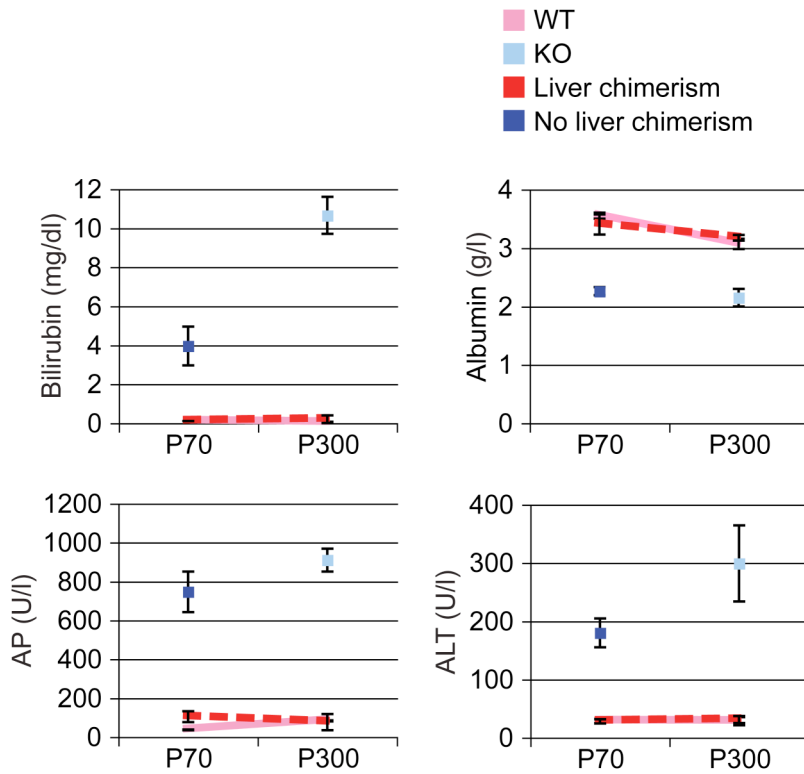
Kidney immunostaining. Frozen sections (10 μm) were stained with goat anti-megalin antibody (Santa Cruz) diluted 1:50, rabbit anti-FAH antibody (gift from Robert Tanguay) diluted 1:15,000 and mouse anti-Ki67 antibody (BD Pharmingen) diluted 1:25. For fluorescent microscopy, primary antibodies were detected with donkey anti-goat antibody conjugated with Alexa Fluor 488, goat anti-rabbit antibody conjugated with Alexa Fluor 594 (both Molecular Probes), diluted 1:500, and the M.O.M. Fluorescein kit (Vector). Nuclear DNA was stained with 2 $\mu\text{g}/\text{ml}$ DAPI (Molecular Probes).

Plasma and urine chemistry analysis. Plasma was diluted 1/4 in 0.9% sodium chloride. Urine was diluted 1/2 in distilled water. Creatinine, AST and glucose concentrations were measured with an ADVIA 1800 (Siemens) chemistry analyzer.

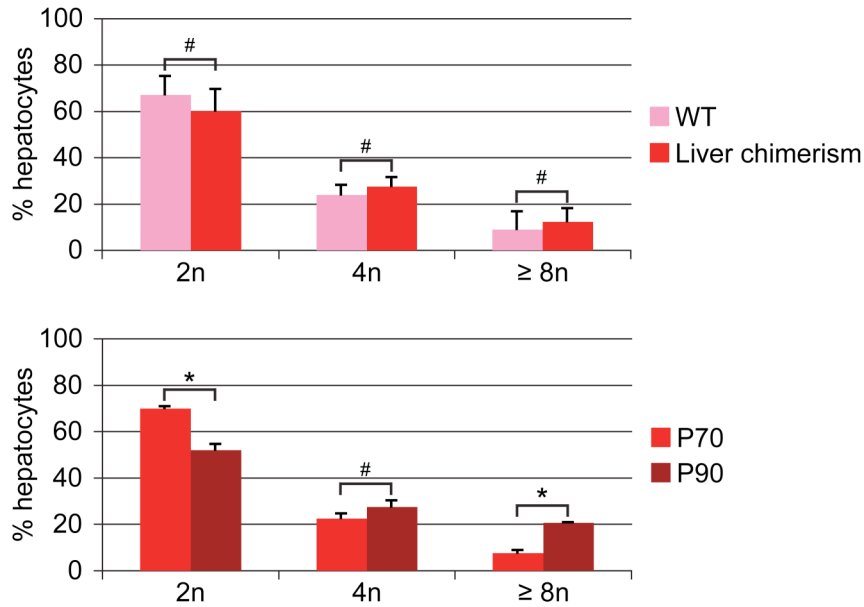
Plasma and urine amino acid analysis. Amino acid concentrations were measured by the Hormone Assay & Analytical Services Core at Vanderbilt University, Nashville, Tennessee, USA. Briefly, 25 μl plasma or urine were added to 25 μl of a solution containing 10% 5-sulfosalicylic acid (EM Science) and 2.5 $\mu\text{mol}/\text{l}$ Norleucine (internal standard). After centrifugation, supernatants were transferred into vials containing 50 μl lithium citrate loading buffer (Biochrom) and loaded onto a refrigerated Biochrom 30 amino acid analyzer.



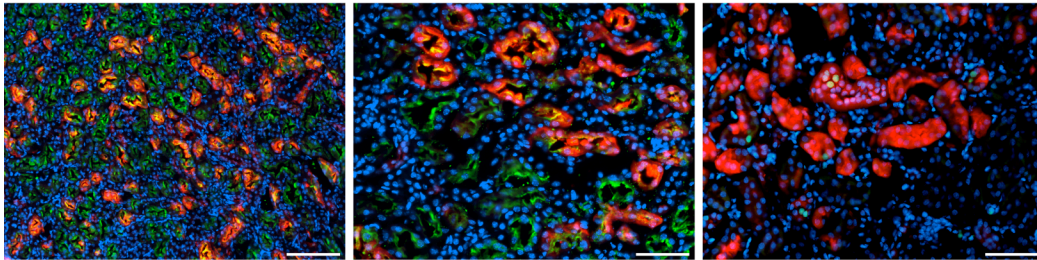
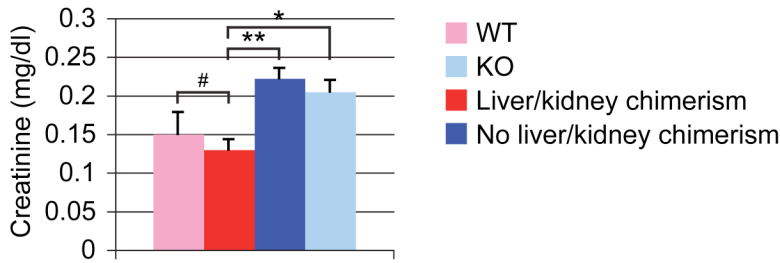
Supplemental Figure 1 Screening for chimeric mice based on contribution of iPS cells to digits. A total of 24 pups were obtained after transfer of 40 iPS cell-injected blastocysts into foster mothers. The iPS cells were homozygous wild-type (WT) while the blastocysts were homozygous knockout (KO) for *Fah*. Pups with high, low or no iPS cell contribution to the digits were identified by simultaneous, semi-quantitative PCR analysis of WT and KO *Fah* alleles in genomic DNA.



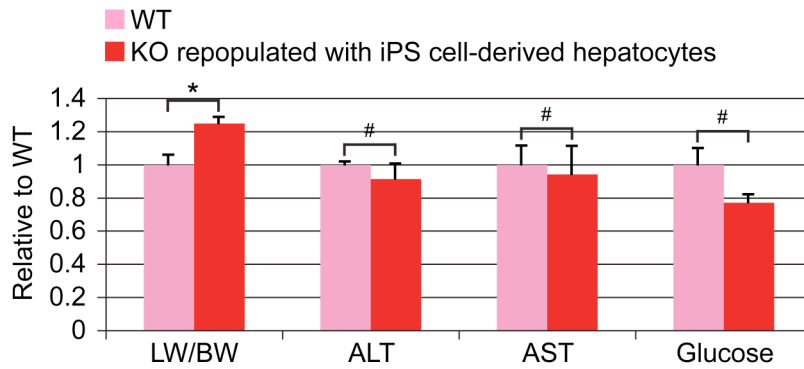
Supplemental Figure 2 Blood analysis of liver function parameters in mice off NTBC at P70 and P300. Mice with liver chimerism were continuously off NTBC since P6. Mice with no liver chimerism or KO mice were placed back on NTBC after the initial blood analysis at P22 but were taken off NTBC again 4 weeks prior to the re-analysis at P70 and P300. Data represent mean \pm SEM. The differences between WT mice/mice with liver chimerism and KO mice/mice with no liver chimerism are highly significant ($P < 0.005$) at both time points. The differences between WT mice and mice with liver chimerism are insignificant ($P > 0.05$) at both time points.



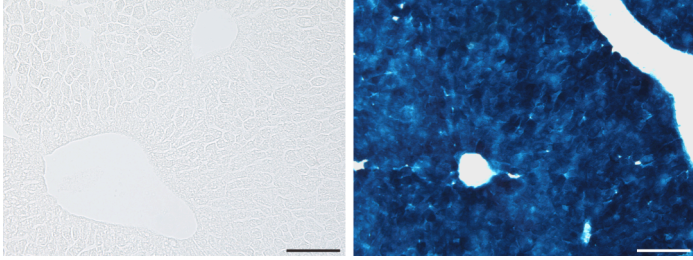
Supplemental Figure 3 Hepatocyte ploidy analysis. Hepatocyte nuclei in liver sections from 3 mice fully repopulated with iPS cell-derived hepatocytes at P70 (Liver chimerism) show the same ploidy distribution pattern as hepatocyte nuclei in 3 age-matched WT mice (upper panel). Comparison of hepatocyte ploidy between a chimeric mouse at P70 and a chimeric mouse at P90 shows that polyploidization of iPS cell-derived hepatocytes progresses further with age (lower panel). Since multinucleated cells were excluded from the analysis, the number of polyploid hepatocytes is underestimated in all mice. At least 150 hepatocyte nuclei were analyzed for each mouse. Data represent mean \pm SEM. * $P < 0.05$; # $P > 0.05$.



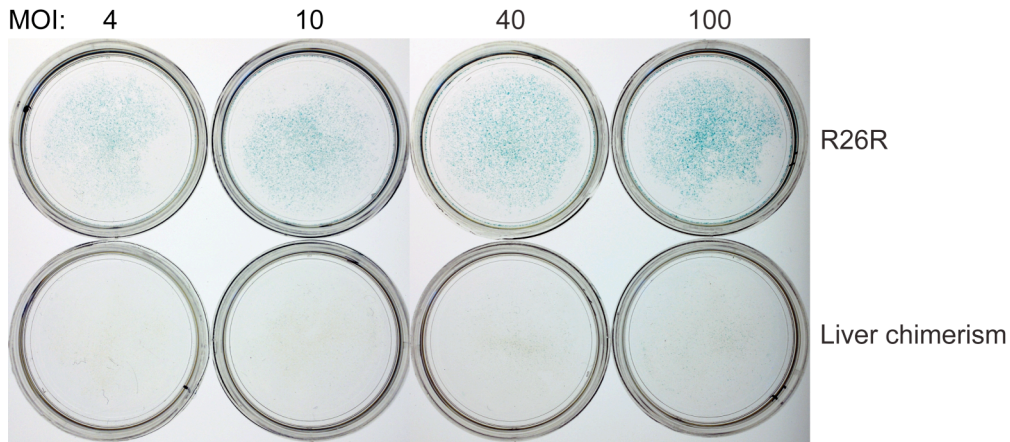
Supplemental Figure 4 Kidneys repopulated with iPS cell-derived proximal tubular cells provide normal function. Chimeric mice have normal plasma creatinine (upper panel) and normal urine amino acids levels (Supplemental Table 2). Co-staining for megalin (green), a scavenger receptor located in the apical membrane of renal proximal tubular cells, and FAH (red) shows that more than 50% of the proximal tubular cells of a representative chimeric mouse are derived from iPS cells (lower panel, left and middle image, low and high magnification). Several iPS cell-derived proximal tubular cells co-express FAH (red) and Ki67 (green, lower panel, right image), indicating that they can proliferate in response to the tubulopathy caused by FAH deficiency. Nuclei are stained blue. Size bars: 100 μm (left image) or 25 μm (other images). Data represent mean \pm SEM. $**P < 0.005$; $*P < 0.05$; $\#P > 0.05$.



Supplemental Figure 5 Analysis of parameters of liver growth and function after two-thirds partial hepatectomy. The ratio of liver weight to body weight (LW/BW) and the levels of ALT, aspartate aminotransferase (AST) and glucose in the blood were measured in 3 WT mice and 3 FAH-deficient mice fully repopulated with transplanted iPS cell-derived hepatocytes 48 hours after two-thirds partial hepatectomy. The results show that iPS cell-derived hepatocytes restore the liver mass as efficiently as WT hepatocytes and are similarly stress-resistant (ALT and AST) and capable of maintaining metabolic liver function (Glucose). The LW/BW is slightly increased in FAH-deficient mice fully repopulated with transplanted iPS cell-derived hepatocytes. The underlying increase in LW is not due to enhanced proliferation of iPS cell-derived hepatocytes after two-thirds partial hepatectomy (Figure 3, B and C) but is regularly observed after liver repopulation (also with WT hepatocytes) in adult FAH-deficient mice (data not shown). Data represent mean \pm SEM. * $P < 0.05$; # $P > 0.05$.



Supplemental Figure 6 Hepatocytes of Rosa26 mice can be reliably detected with X-gal staining. In contrast to a WT mouse (left image), all hepatocytes appear blue after X-gal staining of a liver section from a Rosa26 mouse (right image) used as hepatocyte donor for the competitive liver repopulation experiment described in Figure 3D. Size bars: 100 μm .



Supplemental Figure 7 Visualization of blastocyst-derived hepatocytes rules out cell fusion as the mechanism underlying hepatocyte differentiation of iPS cells free of foreign DNA. Hepatocytes isolated from a R26R heterozygous mouse (R26R) and a chimeric mouse with ~90% liver repopulation (Liver chimerism) were infected with a Cre-expressing adenovirus at increasing multiplicity of infection (MOI). At MOI 10, 40 and 100, 100% of 400,000 plated R26R hepatocytes stained X-gal positive (blue), indicating R26R activation. In contrast, less than 10% of 400,000 hepatocytes isolated from the chimeric mouse were blue. Since the blastocysts used to generate the chimeric mice were both FAH-deficient and R26R heterozygous and the chimeric mouse was repopulated with FAH-expressing hepatocytes to ~90%, this result shows that normal hepatocytes in chimeric mice did not derive from fusion of iPS cell-derived cells with blastocyst-derived hepatocytes. Figure 4A shows sections of the MOI 100 dishes at high magnification.

Supplemental Table 1 Plasma amino acid levels.

Mice	KO		No liver chimera		Liver chimera		WT		KO/ Liver chimera	No liver chim./ Liver chimera	Liver chim./ WT	WT/ KO	WT/ No liver chimera
	4 wks off		4 wks off		10 mths off		off						
Statistics	Mean	SEM	Mean	SEM	Mean	SEM	Mean	SEM	P values				
Threonine	779.4	74.8	533.4	42.9	195.6	14.8	160.8	8.9	4.1E-06	1.1E-05	6.7E-02	2.0E-06	1.4E-06
Serine	810.4	61.2	656.7	108.5	156.4	9.2	134.8	14.0	2.0E-07	7.3E-05	2.2E-01	1.9E-07	6.6E-05
Asparagine	355.4	48.0	215.4	23.8	61.5	9.3	64.9	9.2	3.4E-05	7.1E-05	8.0E-01	3.7E-05	7.9E-05
Glutamic acid	317.0	24.3	315.7	72.2	77.6	23.9	38.4	8.4	4.7E-05	3.3E-03	1.5E-01	2.3E-07	2.9E-04
Glutamine	3835.3	593.2	860.7	68.1	512.2	34.3	484.2	31.6	5.4E-05	9.1E-04	5.6E-01	5.0E-05	4.0E-04
Glycine	571.8	55.1	434.9	32.5	229.8	12.9	234.5	23.1	3.5E-05	8.9E-05	8.6E-01	9.1E-05	1.3E-03
Alanine	2673.6	389.6	1460.8	169.7	522.8	48.3	573.8	126.9	6.7E-05	8.1E-05	7.1E-01	1.6E-04	4.3E-03
Citrulline	77.1	6.4	109.6	14.9	56.9	3.7	44.0	4.6	1.5E-02	1.2E-03	4.9E-02	1.6E-03	4.7E-04
Valine	381.0	63.6	388.4	61.1	226.1	18.4	272.6	20.0	2.2E-02	8.6E-03	1.1E-01	9.2E-02	4.4E-02
Cysteine	49.1	18.1	39.2	23.6	18.2	5.9	36.3	9.1	1.2E-01	2.9E-01	1.5E-01	5.3E-01	9.0E-01
Methionine	449.2	120.1	139.7	31.6	94.2	7.5	76.3	5.9	5.4E-03	7.7E-02	8.5E-02	4.0E-03	1.7E-02
Isoleucine	136.6	21.0	150.1	16.2	93.7	9.2	116.3	11.7	6.6E-02	1.3E-02	1.6E-01	3.9E-01	1.5E-01
Leucine	271.2	57.0	249.4	30.4	156.2	20.8	183.3	12.0	5.8E-02	3.9E-02	2.8E-01	1.1E-01	3.7E-02
Tyrosine	763.3	68.5	434.7	61.4	98.4	8.7	90.6	14.6	4.5E-07	2.8E-05	6.6E-01	5.3E-07	4.9E-05
Phenylalanine	151.6	38.9	84.6	2.9	66.3	1.6	64.5	7.3	2.5E-02	3.8E-04	8.2E-01	2.7E-02	1.3E-01
Ornithine	484.7	75.8	272.6	86.5	95.6	12.9	90.5	18.1	1.4E-04	1.3E-02	8.2E-01	1.5E-04	1.6E-02
Lysine	632.5	143.8	400.6	41.8	293.2	19.1	275.6	17.8	1.9E-02	2.6E-02	5.1E-01	1.5E-02	1.1E-02
1-Methyl-histidine	1.7	0.2	6.8	1.8	6.4	2.0	7.9	1.1	7.4E-02	9.0E-01	5.3E-01	6.9E-04	6.3E-01
Histidine	366.9	38.0	351.8	110.7	70.5	2.8	71.7	6.1	3.0E-06	3.0E-03	8.6E-01	3.8E-06	3.2E-03
Tryptophan	65.1	9.5	54.4	5.9	81.0	7.7	79.5	6.8	2.2E-01	6.8E-02	8.9E-01	2.3E-01	5.9E-02
Arginine	358.8	72.2	144.4	22.7	112.7	13.5	89.7	10.8	2.7E-03	2.5E-01	2.1E-01	1.4E-03	3.7E-02
Proline	280.8	36.1	291.0	51.5	135.2	22.8	95.4	16.1	5.0E-03	1.1E-02	1.8E-01	4.1E-04	1.2E-03

Amino acid levels in $\mu\text{mol/l}$. Abbreviations: KO = Knockout, WT = Wild-type, wks = weeks, mths = months, chim. = chimera.

Supplemental Table 2 Urine amino acid levels.

Mice NTBC	KO		Liver chimerism		WT		KO/ Liver chimerism	Liver chimerism/ WT	WT/ KO
	4 wks off		10 mths off		off				
Statistics	Mean	SEM	Mean	SEM	Mean	SEM	P values		
Threonine	10.088	1.585	0.208	0.023	0.244	0.019	7.2E-04	3.0E-01	3.6E-03
Serine	5.251	0.997	0.127	0.013	0.122	0.009	1.7E-03	8.0E-01	7.0E-03
Asparagine	1.745	0.485	0.127	0.008	0.095	0.006	1.1E-02	3.3E-02	2.8E-02
Glutamic acid	0.375	0.001	0.052	0.004	0.037	0.002	1.4E-08	3.1E-02	2.1E-08
Glutamine	27.564	1.658	0.374	0.039	0.264	0.026	6.7E-06	8.4E-02	8.3E-05
Sarcosine	nrd	nrd	0.244	0.048	0.213	0.029		6.3E-01	
Glycine	6.987	2.188	0.415	0.048	0.378	0.028	1.6E-02	5.7E-01	4.0E-02
Alanine	2.399	0.328	0.259	0.033	0.237	0.015	6.1E-04	6.1E-01	2.8E-03
Citrulline	0.173	0.039	0.011	0.001	0.010	0.001	4.5E-03	7.9E-01	1.5E-02
Valine	0.399	0.062	0.083	0.005	0.108	0.018	1.9E-03	1.9E-01	1.1E-02
Methionine	1.657	0.489	0.132	0.024	0.126	0.009	1.4E-02	8.4E-01	3.6E-02
Isoleucine	0.251	0.046	0.011	0.001	0.010	0.003	1.6E-03	7.2E-01	6.7E-03
Leucine	0.594	0.054	0.133	0.017	0.123	0.015	2.5E-04	6.8E-01	1.1E-03
Tyrosine	9.071	1.015	0.191	0.023	0.135	0.016	1.5E-04	1.3E-01	9.6E-04
β-Alanine	0.051	0.009	0.105	0.018	0.139	0.033	6.3E-02	3.9E-01	6.2E-02
Phenylalanine	1.785	0.347	0.242	0.047	0.101	0.009	3.6E-03	5.4E-02	8.7E-03
γ-aminobutyric acid	nrd	nrd	0.188	0.019	0.183	0.016		8.6E-01	
Ethanolamine	nrd	nrd	0.462	0.078	0.179	0.015		2.9E-02	
Ornithine	0.131	0.006	0.049	0.009	0.071	0.011	1.1E-03	1.9E-01	8.9E-03
1-Methylhistidine	0.126	0.027	0.028	0.006	0.028	0.006	9.6E-03	9.4E-01	2.5E-02
Histidine	8.803	1.836	0.072	0.012	0.056	0.006	2.5E-03	3.4E-01	9.2E-03
Tryptophan	0.240	0.132	0.025	0.004	0.038	0.006	1.1E-01	1.1E-01	2.0E-01
3-Methylhistidine	nrd	nrd	0.047	0.005	0.015	0.006		9.6E-03	
Anserine	nrd	nrd	0.374	0.114	0.321	0.026		7.1E-01	
Carnosine	nrd	nrd	0.136	0.036	0.101	0.008		4.5E-01	
Arginine	0.117	0.007	0.054	0.007	0.089	0.011	1.3E-03	3.7E-02	9.3E-02
Proline	0.541	0.151	0.012	0.008	0.021	0.007	9.1E-03	4.5E-01	2.7E-02
Urine creatinine	17.41	2.166	63.55	3.493	61.27	7.308			

Amino acid levels in μmol/mg after normalization to urine creatinine concentrations measured in mg/dl. Abbreviations: KO = Knockout, WT = Wild-type, wks = weeks, mths = months, nrd = not reliably detected.